Acta Astronautica 68 (2011) 1307–1317

Contents lists available at ScienceDirect

Acta Astronautica

journal homepage: www.elsevier.com/locate/actaastro

Optimization of space orbits design for Earth orbiting missions

Ossama Abdelkhalik *, Ahmed Gad

Mechanical Engineering - Engineering Mechanics Department, Michigan Technological University, 815 R.L. Smith Bldg., 1400 Townsend Dr., Houghton, MI 49931, United States

ARTICLE INFO

Article history:
Received 16 June 2010
Received in revised form
9 September 2010
Accepted 9 September 2010
Available online 8 October 2010

Keywords:
Optimal orbit design
Genetic algorithms applications

ABSTRACT

In Earth orbiting space missions, the orbit selection dictates the mission parameters like the ground resolution, the area coverage, and the frequency of coverage parameters. To achieve desired mission parameters, usually Earth regions of interest are identified and the spacecraft is maneuvered continuously to visit only these regions. This method is expensive, it requires a propulsion system onboard the spacecraft, working throughout the mission lifetime. It also requires a longer time to cover all the regions of interest, due to the very weak thrust forces compared to that of the Earth's gravitational field. This paper presents a methodology to design natural orbits, in which the regions of interest are visited without the use of propulsion systems, depending only on the gravitational forces. The problem is formulated as an optimization problem. A genetic algorithm along with a second order gradient method is implemented for optimization. The design process takes into consideration the gravitational second zonal harmonic, and hence allows for the design of repeated Sun-synchronous orbits. The field of view of the payload is also taken into consideration in the optimization process. Numerical results are presented that demonstrates the efficiency of the proposed method.

1. Introduction

In Newtonian mechanics, the natural motion of a spacecraft around the Earth is described by a second order vectorial differential equation, assuming that the spacecraft is attracted only by the Earth, and assuming that the Earth is a perfect sphere [1]. The solution to these differential equations is either a circular, elliptic, parabolic, or a hyperbolic trajectory [2]. The type of the trajectory is determined depending on how we initially place the spacecraft in orbit. The Earth is always at the focus of this conic trajectory. Regardless of the type of the trajectory, it is always possible to describe the orbit of the spacecraft using five parameters [3]. Another parameter is needed to determine the position of the spacecraft on the orbit. A fundamental task in the design process of any space mission is to design the orbit(s) of the spacecraft. Designing an orbit means, then, finding the values for the five orbital elements such that the mission objectives are best achieved [4].

A wide range of applications require that a spacecraft passes over a given number of ground sites. Examples for this type of missions include remote sensing [5], disaster monitoring [6], urban planning [7], natural resources, and ground surveillance missions [8]. In this type of applications, the spacecraft is usually equipped with sensor(s) to take measurements for the ground sites of interest. The spacecraft does not have to visit (pass over) each site exactly; but rather a ground site is considered "visited" if the field of view (FOV) of the sensor covers that ground site, at some point in time [9]. As can be seen from Fig. 1, the orbit selection dictates the coverage area on Earth surface.

For spacecraft at high altitudes, the coverage area is bigger than that of a spacecraft in a low altitude orbit. On

* Corresponding author. Tel.: +1 906 4873503; fax: +1 906 4872822.
E-mail addresses: ooabdelk@mtu.edu (O. Abdelkhalik), ahgadels@mtu.edu (A. Gad).

0094-5765/$ - see front matter © 2010 Elsevier Ltd. All rights reserved.
doi:10.1016/j.actaastro.2010.09.029

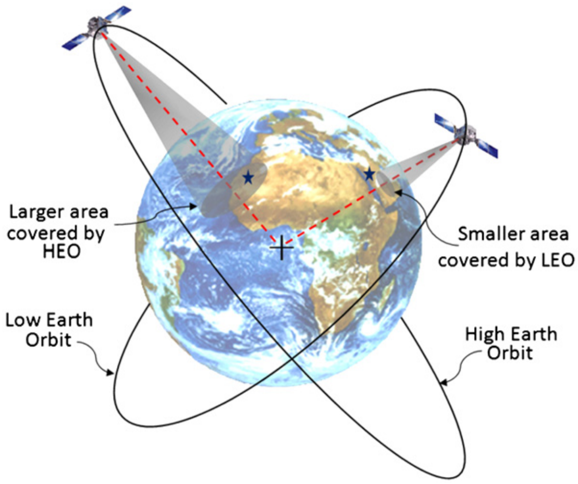

Fig. 1. Spacecraft at high altitudes have larger coverage on Earth as compared to those at lower altitudes.

the other hand, the resolution of measurements from a low altitude spacecraft is better than the resolution that can be obtained from a higher altitude orbit, using the same sensor. The spacecraft orbit also determines the frequency of coverage, which is how often a given ground site will be visited. Besides the coverage area and the ground resolution, there are many other parameters that are affected by the orbit selection, e.g. the size of the spacecraft and the launch cost.

From the preceding discussion, it is clear that there are conflicting objectives that control the selection of the orbit. In many missions, mission designers use propulsion systems, mounted onboard the spacecraft, to maneuver the spacecraft continuously between ground sites. They specify the regions of interest and keep the spacecraft in a low altitude *nominal* orbit. The spacecraft is then controlled to maneuver between the regions of interest using the thrusters. This way, it becomes possible to collect high resolution measurements, and still visit all the ground sites, within a given time frame. There is an important research problem associated with this way of designing the space mission: what is the control strategy such that the fuel expenditure for maneuvering the spacecraft, between ground sites, is minimal. Several studies have addressed this problem. A representative study is the work developed by Guelman and Kogan [10], where they developed an optimal control algorithm to sort the sites in an optimal sense, and then maneuver the spacecraft between them. The results of their study show that the thrusters have to be working continuously throughout the mission lifetime. A typical example that they discussed is the case of 20 ground sites. The results show that a time frame of 50 days is needed to complete visiting all the sites [10]. These solutions have major weaknesses: (1) they require thrusters to work continuously throughout the mission life time. This puts severe demands on the spacecraft systems, in terms of the power and fuel needed to run the thrusters, and hence dramatically increases the mission cost, and (2) this solution requires a longer mission durations, due to the very low thrust level of the electric propulsion systems. For the case of 20 ground sites, the time needed to visit all of the sites is about 50 days using propulsion. If a natural orbit exists, all the sites will be visited in a much smaller time frame. These major weaknesses are mainly because these algorithms use propulsion systems, in some sense, to oppose the natural gravitational forces.

In previous works, a method to design natural orbits, to visit the regions of interest without the use of propulsion, was developed [11]. A spacecraft, in a natural orbit, needs to be as close as possible to Earth when visiting a ground site to achieve high resolution. Yet, a synchronization is needed, between Earth rotational motion (spinning) and the spacecraft motion, to guarantee visiting all the ground sites. To find these natural orbits, two approaches were developed. In the first approach, the problem is formulated as an optimization problem. Stochastic optimization methods were used as an attractive alternative for optimizing space orbits design [12,13]. The cost function for this type of problems usually have numerous local minima. For this specific problem, a genetic algorithm technique was implemented for optimization [14]. The second approach adopted a semi-analytical method to reduce the number of unknowns and then perform numerical search or stochastic optimization [15]. The two methods suffer from the following weaknesses: (1) the two methods assume a two-body model for the spacecraft motion (A two-body model is a model that assumes the spacecraft attracted only by the Earth, which is assumed a perfect sphere. In reality, this is not true. A more accurate model for the Earth gravitational field includes the effect of the Earth oblateness. This effect is modeled as zonal harmonic coefficients known as J 2, J 3, etc.), (2) both methods assume zero field of view for the spacecraft sensor. This assumption limits the number of solutions to the problem, and (3) the semi-analytical method assumes the existence of a solution. If a perfect solution does not exist, the method cannot return any solution even if there exists a solution with a small error. In recent developments, Kim et al. investigated the possibility of using a genetic algorithm for finding the temporary target orbit, in order to reduce the average revisit time of an existing mission orbit, over a particular target site during a given time window [16]. Genetic algorithms are also used to optimize the fuel consumption of low Earth orbit constellations for temporary reconnaissance missions [17], and also to minimize telecommunications coverage blackouts [18].

This paper addresses the problem of optimal orbit design taking into consideration the second zonal harmonic of the Earth gravitational field, and taking into consideration the field of view of the sensor on board of the spacecraft. Taking the gravitational perturbations into consideration in the optimization process allows for the design of repeated ground track sun-synchronous orbits. This type of orbits makes the spacecraft visits the same Earth site every given number of days, at the same day-time. On the other hand, taking the sensor's FOV into consideration in the optimization process results in more feasible solutions. A standard optimization tool that carries out coverage calculations is usually computationally expensive.

The algorithm presented in this paper reduces the computational cost, while carrying out an optimization process, in two aspects: (1) the development in this paper benefits from analytical developments to reduce the number of independent variables. A genetic algorithm is then developed to select the independent variables, in an optimal sense. The reduced number of independent variables leads to faster convergence and a reduced number of objective function evaluations, and (2) a fast numerical algorithm is developed to roughly compute the coverage state of a ground site. It is rough in the sense that it assumes that J 2 is the only perturbing effect from the two-body model.

Several objective functions can be used. In this paper, an objective function that maximizes the number of visited ground sites and minimizes the time frame needed for the mission is presented. The problem formulation is presented in Section 2. Section 3 presents the developed solution algorithm, focusing on the underlying physics and the analytical relations between the variables. The developed optimization tool is described in Section 3.5, where the implementation of the genetic algorithm and the selection of its parameters are briefed. Section 4 presents the results for one case study.

2. Problem formulation

Given a set of ground sites, defined by the longitude and latitude for each ground site, the right ascension, ϕ_i for each site can be computed at any time. It is desired to find a natural orbit solution on the pareto front solutions such that the field of view of the spacecraft covers the maximum number of sites, from the given set, while minimizing the mission time frame. The J_2 gravitational zonal harmonic is included in the dynamic model.

For a certain candidate orbit plane, as Earth completes one revolution about its spinning axis, each site intersects the orbit plane twice. If, at the intersection time, the spacecraft's FOV does not cover the ground site, then the site is not visited at that time. A site will be visited if, and only if, at the intersection time, the spacecraft's FOV covers the site.

Therefore, the problem may be formulated as follows: given a set of ground sites and a time frame for visiting them, find the orbit that visits the maximum number of sites, where visiting a ground site is defined as such for each ground site, at one of its intersections with the orbit plane, it is within the spacecraft's FOV, in a minimum time frame. Therefore, the fitness function F_i is defined as

$$F_i = f_1 \frac{(J_{1_i})^{f_2}}{(J_{2_i})^{f_3}} \tag{1}$$

where f_1, f_2, and f_3 are weight parameters, and J_{1_i} and J_{2_i} are the fitness terms for the ith design point which are defined as

$$J_{1_i} = N, \quad J_{2_i} = m \tag{2}$$

where N is the total number of covered sites in m days, and m is the ground track repetition period in days. N is a dependant variable that can be computed given the candidate orbit and the set of sites to select from. The values of the fitness weight parameters f_1, f_2, and f_3 determines the relative importance of maximizing the number of covered sites versus minimizing the mission time frame.

3. Optimization

A genetic algorithm is developed to solve this problem. The unknown variables are the five orbital elements and the visiting times of all the ground sites. So, the total number of unknowns is $N+5$, where N is the number of ground sites. A standard genetic algorithm would lump all the unknown variables in one chromosome, generate a random initial population, and use genetic operations (e.g. crossover and mutation) to generate subsequent generations of the population. In this problem, however, a direct application of a standard genetic algorithm would suffer from the following weakness: the evaluation of the fitness of a candidate solution (member) requires running a simulation for the spacecraft motion for the whole time frame specified in the problem. During this simulation, a coverage calculation function is used to assess the quality of the solution (which ground sites are visited and when.) This simulation is computationally expensive. To make the optimization tool computationally more efficient, we developed the following algorithm that benefits from the physics of this particular problem to reduce the number of design variables and to reduce the coverage calculations time.

The solution algorithm has only four independent variables. The physics of the problem along with the constraint equations are used to compute the rest of the unknown quantities. The inclusion of the constraints and physics of the problem, to reduce the number of independent variables, has two advantages: (1) it reduces the number of design variables, and (2) it guarantees that each member in the design space is a feasible solution (feasible orbit.) A feasible orbit is a solution orbit that satisfies all the physics of the problem as well as the problem constraints. This approach, in fact, reduces the size of the design space. Based on the equations that describe the problem physics and constraints, the design variables are selected to be the eccentricity e, the inclination i, the spacecraft's true anomaly above the first ground site ϑ_1, and the ground track repetition period in days, m. The selection of ϑ_1 among the design variables guarantees that the candidate orbit covers at least one of the specified ground site. Selecting e and i to be design variables gives flexibility in designing Sun-synchronous orbits. For each feasible orbit, all given ground sites are checked whether they are visited during the m days or not, as illustrated in Fig. 2. Section 3.1 briefs the constraints of having a repeated ground track and Sun-synchronous orbit. Section 3.2 briefs the physics of computing two unknown quantities (the argument of perigee and the right ascension of ascending node) from the design variables. Section 3.3 also briefs the physics of computing the luci of the ground sites when they are visited by the spacecraft, from the design variables.

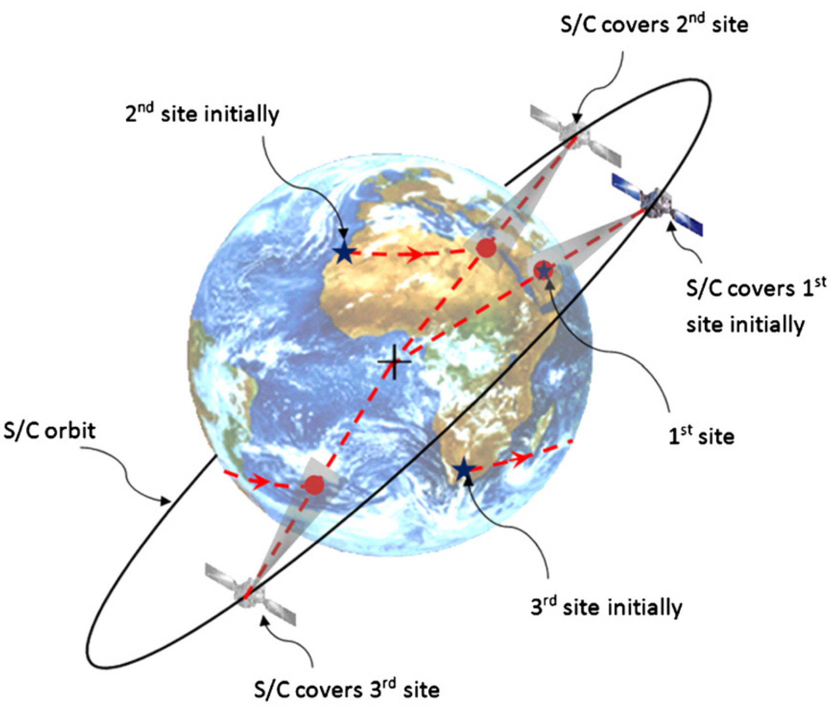

Fig. 2. Spacecraft trajectory covers three ground sites.

Section 3.4 presents the coverage calculations implemented in this work. Sections 3.1–3.4 are preparations for implementing the genetic algorithms. Section 3.5 describes the implementation of genetic algorithms.

3.1. Sun-synchronous repeated ground track orbit

For a given set of values for the four design variables (member in the design space), the orbit semi-major axis, a, is constraint to be [19]

$$a=\left[-\frac{3R_E^2 J_2\sqrt{\mu}}{2(1-e^2)^2\dot{\Omega}}\cos i\right]^{2/7} \quad (3)$$

where $\dot{\Omega}=1.991\times10^{-7}$ rad/s is the desired rate of change of the orbital right ascension of the ascending node, in order to have a Sun-synchronous orbit. The constraint of having a repeated ground track orbit can be formulated as follows [9]:

$$n|\Delta\phi|=2\pi m \quad (4)$$

where n is the total number of successive orbit revolutions performed, m is the number of Earth revolutions (in days) before the ground track repeats itself, and $\Delta\phi$ is the total changes in longitude after one nodal period. $\Delta\phi$ is defined as [9]

$$\Delta\phi=\Delta\phi_1+\Delta\phi_2 \text{ rad/orbit} \quad (5)$$

where $\Delta\phi_1$ and $\Delta\phi_2$ are the change in longitude due to the Earth's rotation and the regression of the line of node, respectively. They are computed as follows [9]:

$$\Delta\phi_1=-2\pi\frac{\tau}{\tau_E} \text{ rad/orbit} \quad (6)$$

$$\Delta\phi_2=-\frac{3\pi J_2 R_E^2\cos i}{a^2(1-e^2)^2} \text{ rad/orbit} \quad (7)$$

where τ_E is the Earth's sidereal rotational period ($\tau_E=86164.1$ s), and τ is the spacecraft's nodal period. For a Sun-synchronous orbit, the required rotation rate, $\Delta\phi_2$, is [9]

$$\Delta\phi_2=2\pi\frac{\tau}{\tau_{ES}} \text{ rad/orbit} \quad (8)$$

where $\tau_{ES}=3.155817\times10^7$ s is the orbital period of the Earth orbit around the Sun. Nodal period (node-to-node τ) can be defined as [20]

$$\tau=\frac{2\pi}{n+\dot{M}_0+\dot{\omega}} \quad (9)$$

where n is the orbital mean motion, M_0 is the initial mean anomaly, and ω is the argument of perigee. Due to J_2 perturbation, the time rate of change of M_0 and ω are [20]

$$\dot{M}_0=\frac{3nJ_2[3\cos^2 i-1]}{4(1-e^2)^{3/2}}\left(\frac{R_E}{a}\right)^2 \quad (10)$$

and

$$\dot{\omega}=-\frac{3nJ_2[1-5\cos^2 i]}{4(1-e^2)^2}\left(\frac{R_E}{a}\right)^2 \quad (11)$$

The above two constraints are implemented as follows. First, all the design variables are selected by the optimization tool. Then, the semi-major axis is computed using Eq. (3) to generate a Sun-synchronous orbit. This solution, however, does not yet satisfy the repeated ground track constraint (Eq. (4)). For any orbit, it is possible to slightly tune its inclination to obtain a repeated ground track orbit which is very close to the untuned orbit [21]. Therefore, the inclination value is numerically tuned in order to generate a Sun-synchronous repeated ground track orbit satisfying the problem constraints. Tuning the inclination value leads to a considerable change in the semi-major axis value according to Eq. (3).

3.2. Computation of the right ascension of ascending node and argument of perigee

At this point, the unknown orbital elements are the argument of perigee, ω, and the right ascension of the ascending node, Ω. The spacecraft is assumed, without loss of generality, to be initially above the first site, i.e. the first site is on the spacecraft's nadir point. So, a unit vector $\hat{r}_1$ in the direction of the first site can be determined as follows:

$$\hat{r}_1 = [\cos\lambda_1\cos\phi_1, \cos\lambda_1\sin\phi_1, \sin\lambda_1]^T = [r_{1x}, r_{1y}, r_{1z}]^T \tag{12}$$

where ϕ_1 and λ_1 are the latitude and longitude of the first site, respectively. Then, given the known orbital elements, the spacecraft position vector $\vec{r}_1$ can be calculated as [19]

$$\vec{r}_1 = \frac{a(1-e^2)}{1+e\cos\vartheta_1}\hat{r}_1 \tag{13}$$

Since $\vec{r}_1$ is in the orbit plane and the inclination is fixed, then, geometrically, there is only two possible values for the right ascension of the ascending node, Ω. To better see this, consider the special case of an inclination of 90° and $\hat{r}_1$ in the inertial Y–Z plane. There are two possible orbit planes, the normals of which are $\hat{h}_1$ and $\hat{h}_2$ in Fig. 3. From Fig. 3, we can see that there are two possible values for Ω, the values of which are $\pi/2$ and $3\pi/2$. In general, to calculate the two possible values of Ω, the transformation of the vector $\vec{r}_1$ from the inertial frame (ECI) to the perifocal frame (PQW) is considered [19]

$$\vec{r}_{1_{PQW}} = R_3(\omega)R_1(i)R_3(\Omega)\vec{r}_{1_{ECI}} \tag{14}$$

where $\vec{r}_{1_{ECI}}$ is calculated from Eq. (13), and $\vec{r}_{1_{PQW}}$ can be calculated as follows:

$$\vec{r}_{1_{PQW}} = r_1[\cos(\vartheta_1), \sin(\vartheta_1), 0]^T \tag{15}$$

where $r_1 = \|\vec{r}_1\|$. Eliminating r_1 from both sides of Eq. (14) and considering only the third row, then

$$r_{1x}\sin(i)\sin(\Omega) - \sin(i)\cos(\Omega)r_{1y} + \cos(i)r_{1z} = 0 \tag{16}$$

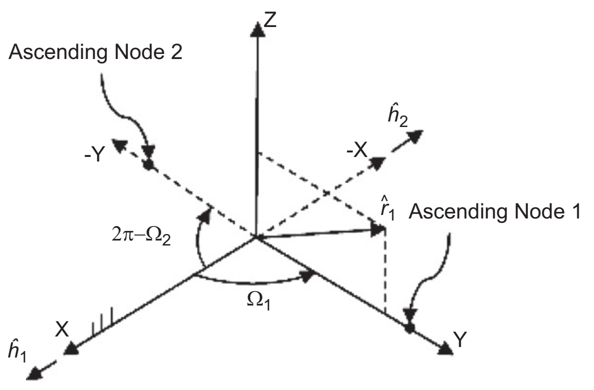

Fig. 3. Two possible locations for the ascending node, for given $\hat{r}_1$ and i.

The only unknown in Eq. (16) is Ω and its solution yields two values for Ω. Eq. (16) could be solved analytically and its closed form solution is as follows [22]:

$$r_{1x}\sin(i)\sin(\Omega) - \sin(i)\cos(\Omega)r_{1y} = R\cos(\Omega-\alpha) \tag{17}$$

where $R = \sqrt{(-r_{1y}\sin(i))^2 + (r_{1x}\sin(i))^2}$ and $\alpha = r_{1x}/(-r_{1y})$

$$R\cos(\Omega-\alpha) = -\cos(i)r_{1z} \tag{18}$$

Therefore, Eq. (18) can be solved to obtain the two possible planes for the orbit (i,Ω_1) and (i,Ω_2).

Next we calculate the argument of perigee, ω. Given that the orbit plane is fixed, and since the true anomaly of the spacecraft when it is above site 1 is known (θ_1), and the direction to the spacecraft position at that point is known $(\hat{r}_1)$, then there are two possible directions for the eccentricity vector in each orbit plane. These two directions are $(\pm\theta)$ around $\hat{r}_1$ in the orbit plane, as shown in Fig. 4. From Fig. 4, the two possible directions for the $\hat{e}$ correspond to two different directions for the spacecraft motion. Since for each orbit plane, the direction of spacecraft motion is fixed, then one of the two values for ω is rejected, see Fig. 4. This leaves one possible value for ω in each orbit plane.

3.3. Computation of intersection locations

To complete the algorithm, we need to develop a method to check whether all target sites are visited within the given time frame or not, for a candidate orbit solution. The longitude ϕ and the latitude λ for each ground site are given. At any point in time, a ground site is not, in general, in the spacecraft's orbit plane; and hence, at this time, it is not being visited. As Earth is spinning, each ground site moves on a circle normal to the Earth axis of rotation, which is the constant declination circle of that site, as shown in Fig. 5. For each site, the latitude circle (same as the constant declination circle) intersects with the spacecraft orbit plane twice, in one orbital revolution. Due to Earth spinning and J_2 effect, the intersection location coordinates, for a given site, change over time, from one orbit revolution to the other. To check whether, or not, a ground site is visited, in the given time frame, all of its intersection points, with the candidate orbit plane, need to be accurately calculated, over the whole time frame. The site is considered visited if at least one of the intersection points is in the instantaneous coverage region of the spacecraft, at the intersection time.

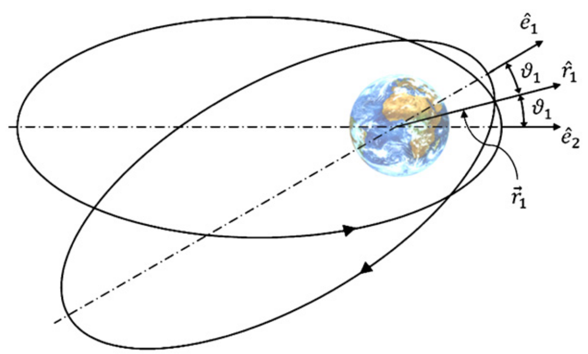

Fig. 4. Two possible orbit orientations in the orbit plane, for given $\vec{r}_1$ and $\vec{r}_{ij}$.

To simplify the calculations of the intersection locations, we do it on two steps. First, the intersection locations are approximately calculated assuming a two-body motion. Then a numerical correction is applied to determine the correct intersection locations, for each site. In a two-body motion, the orbit plane is fixed over time. Therefore, all the orbital elements, but the true anomaly, are constant over time. With this assumption, we can use a closed form solution to find the intersection points. The closed form method is explained in the appendix. Two intersection locations are calculated, see Fig. 5.

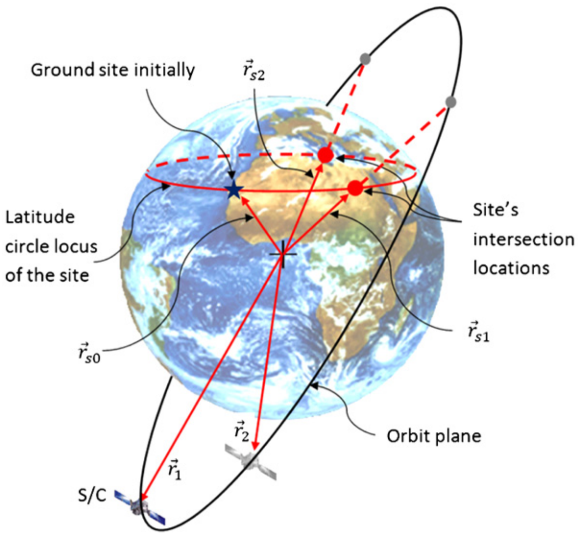

Fig. 5. Two intersection locations of a fixed two-body orbit plane with the latitude locus circle of a ground site.

Due to J_2 perturbation, the orbit plane changes over time. Hence, a correction is needed for the intersection locations. A numerical scheme is developed to achieve this correction. An iterative approach is implemented to calculate the time at which the site intersects with the rotating orbit plane. Fig. 6 explains the idea of this scheme. First, the spacecraft is propagated from $\vec{r}_1$ to a new position vector, $\vec{r}_2$. The propagation is for a guessed value for the time until intersection Δt, or for the true anomaly change, ϑ_{12}. The J_2 perturbation effect is taken into consideration in spacecraft propagation. The plane defined by the vectors $\vec{r}_1$ and $\vec{r}_2$ is an initial approximation for the orbit plane. This plane and the initial position vector of the site, $\vec{r}_{s0}$, are used to calculate the intersection position vectors, $\vec{r}_{s1}$ and $\vec{r}_{s2}$, using the closed form method presented in the appendix. This completes the first iteration.

A new update for the time interval Δt between the initial site location $\vec{r}_{s0}$ and its intersection location $\vec{r}_{sj}$ with the orbit plane is calculated, as illustrated in Fig. 7. Δt can be calculated as follows:

$$\Delta t = \frac{|\Delta\phi_{sj}|}{\omega_E} \tag{19}$$

where ω_E is the Earth spinning rate ($\omega_E = 7.2921 \times 10^{-5}$ rad/s), and $\Delta\phi_{sj}$ is the change in site longitude due to Earth spinning, and is defined as

$$\Delta\phi_{sj} = \phi_{sj} - \phi_{s0} \tag{20}$$

where ϕ_{s0} is the site's initial right ascension, and ϕ_{sj} is the intersection location right ascension. The latter can be calculated as follows:

$$\phi_{sj} = \tan^{-1}\left(\frac{\vec{r}_{sj}(2)}{\vec{r}_{sj}(1)}\right) \tag{21}$$

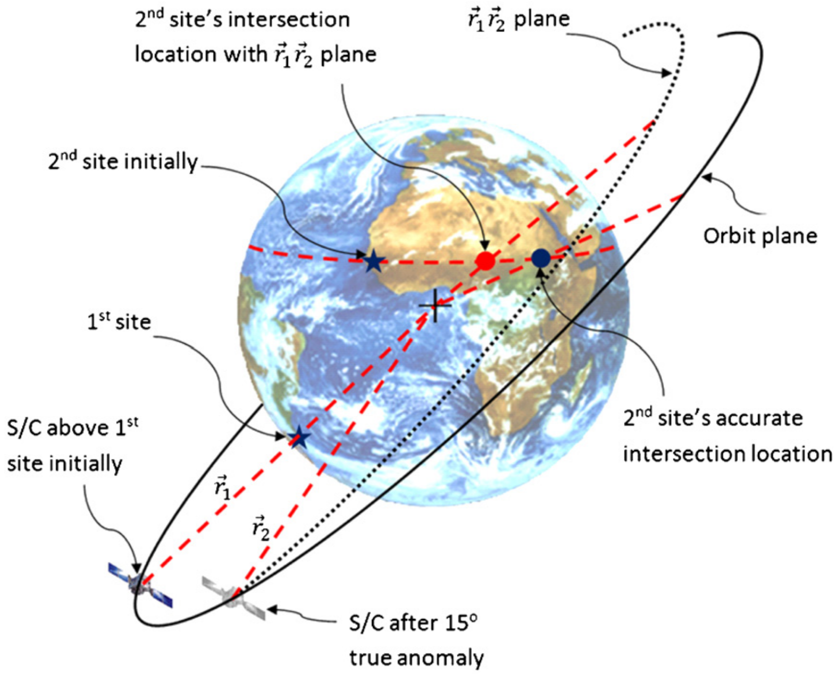

Fig. 6. Ground site's intersection locations with spacecraft perturbed trajectory.

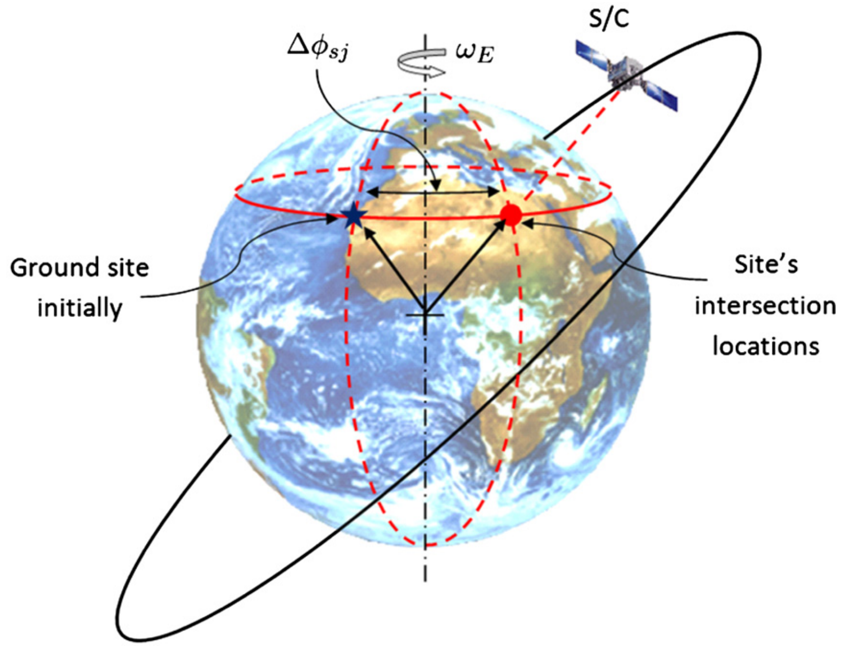

Fig. 7. The change in site longitude due to Earth spinning.

Using the updated value of Δt, the new orbit plane is calculated by propagating the vectors $\vec{r}_1$ and $\vec{r}_2$ by Δt. A more accurate approximation for the orbit plane is obtained. The J_2 effect is taken into consideration in propagation. The updated orbit plane and $\vec{r}_{s0}$ are used to calculate a new update for the intersection locations, using the algorithm in the appendix. The procedure is repeated until no improvements can be obtained. New intersection locations are computed, for each day in the given time frame m. So, there are $2m$ intersection points between the orbit plane and each site, within m days time frame. Recall that at each design point, we have two possible orbit planes.

At this step, we know the times at which the sites intersect with the orbit plane. The next step is to check whether each sites will be covered by the spacecraft or not, at the times of intersections. If all sites are covered, then the candidate orbit is a solution orbit. The next section briefs how to calculate the coverage for a site.

3.4. Coverage with sensor's FOV

The field of view (FOV) of the spacecraft is defined as the angular distance viewed by the instrument installed on the spacecraft. Fig. 8 shows the definitions and angular relationships between the spacecraft, Earth's center, and coverage zone. The angular radius of the Earth ρ and the maximum Earth central angle λ_0 can be calculated from the geometric relation:

$$\sin\rho = \cos\lambda_0 = \frac{R_E}{R_E + H} \tag{22}$$

The nadir angle η (also called half of the angular FOV) is measured at the spacecraft from the nadir point to the end of coverage zone. The spacecraft elevation angle ε is the

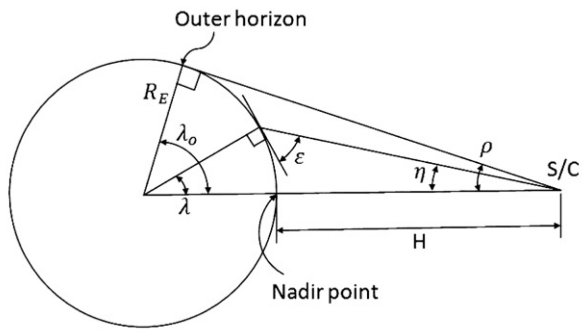

Fig. 8. Definition of angular relationships between the spacecraft, Earth's center, and coverage zone.

angle measured at coverage ending zone between the spacecraft and the local horizontal. Given η, ε can be computed as [4]

$$\cos\varepsilon = \frac{\sin\eta}{\sin\rho} \tag{23}$$

The Earth central angle λ is measured at the center of the Earth from the nadir point to the end of coverage zone. λ can be computed as

$$\lambda = \frac{\pi}{2} - \eta - \varepsilon \tag{24}$$

Let $\vec{r}_{s/c}$ and $\vec{r}_{sj}$ be the spacecraft and site position vector, respectively, at the time we check the coverage. The angle θ_{cov} is the angle between these two vectors, and can be computed as follows:

$$\theta_{cov} = \frac{\vec{r}_{s/c} \cdot \vec{r}_{sj}}{r_{s/c} r_{sj}} \tag{25}$$

If the angle θ_{cov}, for a certain site, is less than or equal to the Earth central angle λ, then this site is covered by the spacecraft, at this time.

3.5. Genetic algorithm implementation

This section describes how we optimize the selection of the independent design variables. The purpose is to design a Sun-synchronous repeated ground track orbit that covers as many sites as possible, from a given set of ground sites, in minimum mission time. The parameters to be optimized are eccentricity e, inclination i, spacecraft's true anomaly above the first ground site ϑ_1, and the ground track repetition period in days, m. The fitness F_i function is calculated according to Eq. (1). In this paper, the weight parameters are selected to be: f_1=1.5, f_2=1, and f_3=0.1. Therefore, the fitness function becomes

$$F_i = \frac{1.5N(e,i,\vartheta_1,m)}{m^{0.1}} \tag{26}$$

To see how the fitness function F_i varies with the change in the design variables, F_i is plotted versus e and i in Fig. 9. In Fig. 9, five ground sites are randomly selected to be the set of ground sites. The field of view (FOV) is selected to be 10°. The other two design variables ϑ_1 and m are selected to be 0° and 10 days, respectively.

The objective function shown in Fig. 9 is a multi-minima function. Classical optimization methods fail to find the optimal solution in this case. On the other hand, genetic algorithms can be implemented to find a highly fit solution for the problem. Genetic algorithms are search algorithms based on the mechanics of nature selection and natural genetics. They combine survival of the fittest among string structures with a structured yet randomized information exchange to form a search algorithm [23].

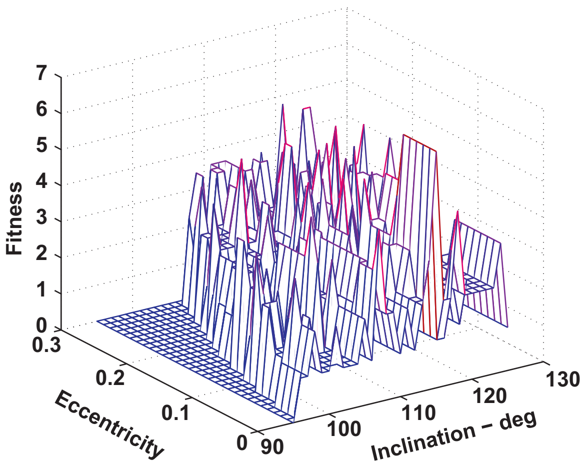

Fig. 9. The fitness function variation versus the orbital elements.

In genetic algorithms, a design point is called a member. A finite number of members are randomly generated to create the initial population. Generations of this population are created using genetic algorithms operations such as reproduction, crossover, and mutation. Each generation is a single iteration. At each generation, members that are fittest are selected in a parent's pool. The fitness of a member is determined according to the objective, the cost function in this case. These parents are then used to create the new generation. This process leads to the evolution of populations of individuals that are fittest.

Each member, design point, in the population represents four design variables. Three of them are the orbital elements that are coded as continuous design variables. These variables are e, i, and ϑ_1. The mission time frame, m, is coded as a discrete design variable. Each member is presented in a binary format as a binary string. This string contains the binary representation of all the design variables values at the corresponding design point. The number of bits for each variable determines its accuracy. Discrete variable would be assigned as a unique binary string. The number of bits q_m for the discrete design variable, m, depends on the upper bounds of the desired design variable, m_{max}, which is specified as an input to the problem. The number of bits, q_m, for the discrete design variable m is determined as follows:

$$q_m = 1 \text{ bit} \quad \text{if } m_{max} = 1 \text{ day}$$

or,

$$2^{q_m} \le m_{max} \quad \text{if } m_{max} > 1 \text{ day} \tag{27}$$

For the continuous design variables, the number of bits q_i for a continuous design variable A_i is selected according to the following inequality:

$$2^{q_i} \le \frac{A_{imax} - A_{imin}}{A_{ic}} + 1 \tag{28}$$

where A_{imin} and A_{imax} are the lower and upper bounds on the ith continuous design variable, and A_{ic} is the desired accuracy. Table 1 shows the values of the lower and upper bounds, accuracy, and number of bits for each continuous design variable. For a Sun-synchronous orbit, the orbit inclination range is limited as shown in Fig. 10. The inclination should be more than 90° to provide the desired regression of nodes of a Sun-synchronous orbit. Also, a limitation on the eccentricity, to be less than 0.6, is

Table 1
The values of the lower and upper bounds, accuracy, and number of bits for each continuous design variable.

Continuous design variable A_i	**Lower bounds** A_{imin}	**Upper bounds** A_{imax}	**Accuracy** A_{ic}	**Number of bits** q_i
Eccentricity e	0	0.6	0.001	10
Inclination i (deg)	90	175	0.001	12
First site's true anomaly ϑ_1 (deg)	0	360	0.001	13

applied to guarantee a certain minimum altitude for the spacecraft.

The strings for all members in the initial population are selected randomly within the design variables limitations. Each member consists of the four design variables. The values of the four design variables are used to evaluate the unknown orbital elements and check the coverage of each ground site. This process is carried out as described in the previous sections. Then, the fitness function F_i, for each member i in the population, is calculated using Eq. (26). The fittest members in the population are selected as parents for the next generation. Genetic algorithm operations are then used to generate a new generation. This process is repeated for a predefined number of generations. Finally, the fittest members in the last generation are selected. The most fit design point is the member which represents a Sun-synchronous repeated ground track orbit that optimizes the objective function.

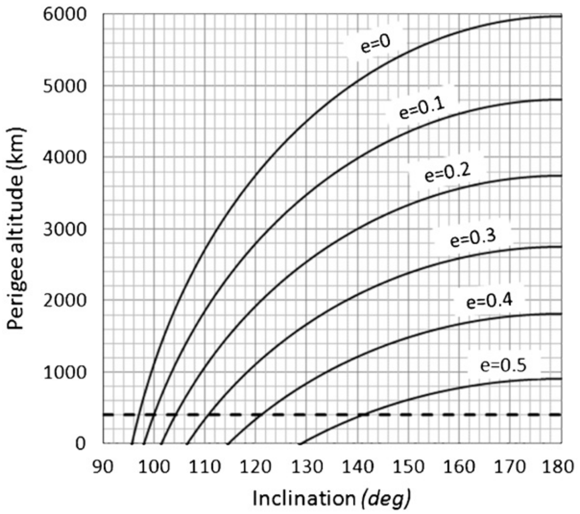

Fig. 10. The orbital elements limitations for a Sun-synchronous orbit.

4. Numerical results

As a challenging numerical example of designing J_2 perturbed orbits, a set of 20 ground sites is randomly selected, as shown in Fig. 11. The field of view (FOV) is selected to be 10°. The ranges of the three independent variables, e, i, and ϑ_1, are chosen according to Table 1. While the maximum possible value for the fourth variable, m, is selected to be 32 days. The population size is selected to be 100, and the number of generations is 200. The probability of crossover is selected to be 0.9, while the mutation probability is in the range of 0.01 and 0.08. The most fit 10% of the members in each generation are copied automatically into the next generation without performing any genetic operations. Eq. (26) is used as the fitness function to be maximized. All of the tests have

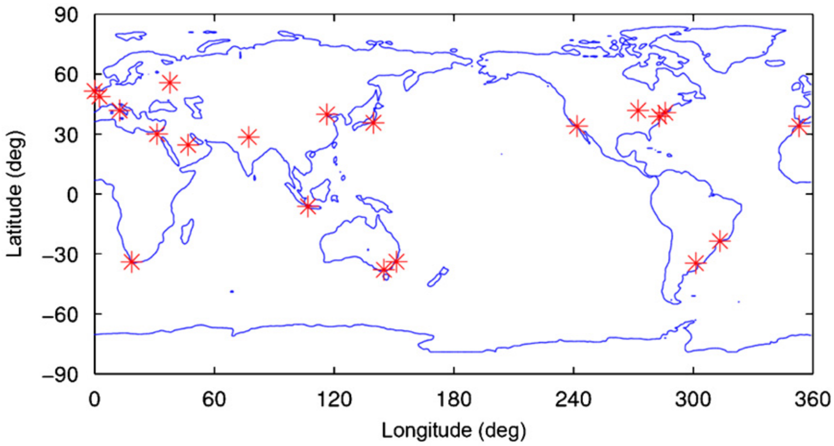

Fig. 11. A set of random 20 ground sites.

Table 2
The orbital elements of a sample of the solutions, for the 20 sites problem.

Orbit parameters	Fittest orbit	Alternative orbits		
Semi-major axis a (km)	10 031.187	10 025.712	9 935.833	11 081.923
Eccentricity e	0.1935	0.1935	0.1419	0.1935
Inclination i (deg)	116.55	116.50	116.62	129.31
Right ascension of ascending node Ω (deg)	263.41	348.60	263.45	344.55
Perigee argument ω (deg)	306.77	79.254	306.84	61.611
True anomaly of the first site ϑ_1 (deg)	141.17	146.82	141.17	141.17
No. of covered sites	20/20	12/20	11/20	9/20
Ground track repetition, period, m (days)	25	17	17	9

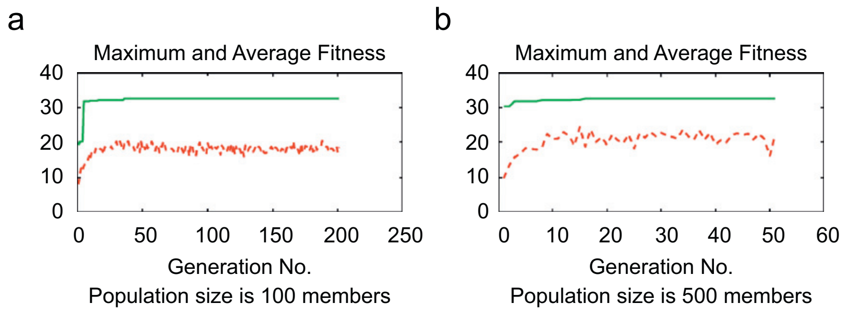

Fig. 12. The convergence of the developed genetic algorithm using two population sizes: (a) 100 and (b) 500.

been performed on a 2.00 GHz Intel Xeon processor with Windows XP.

The fittest orbit obtained by the GA is an orbit that covered the 20 sites in 25 days. The computational time for this case is 12 h. The orbital elements of the fittest solution are listed in Table 2. The developed algorithm can be used to provide many other alternative orbits which cover less number of ground sites in less repetition period. Table 2 shows the orbital elements of a sample of these alternative orbits. To generate these results, several trials have been attempted with different selections for the genetic operations parameters. Fig. 12 shows the convergence of the algorithm for two different population sizes.

5. Conclusion

In this paper, the problem of initial orbit design for regional coverage, using natural (no thrust) orbits, is investigated. A novel problem formulation is developed to design an orbit that covers as many ground sites as possible, from a given set, while minimizing the mission time frame. The J_2 perturbation effect is implemented as a constraint to guarantee Sun-synchronous repeated ground track orbit solutions. The spacecraft's field of view is an input parameter to the developed algorithm. The developed method demonstrated success in finding fit solutions for challenging case studies. One useful feature about implementing the genetic algorithms in optimization is that it provides several solutions to the problem, presenting different interesting features. The implementation of the developed algorithm in constellations design is a future research topic.

Appendix A. Position vectors of ground sites at their intersections with an orbit plane

Given two spacecraft position vectors $\vec{r}_1$ and $\vec{r}_2$ at two different times, and a site position vector $\vec{r}_{s0}$ at initial time. The vectors $\vec{r}_1$ and $\vec{r}_2$ define the orbit plane. The position vectors of the target site at the times it intersects with the orbit plane are $\vec{r}_s$. Since the vectors $\vec{r}_1$, $\vec{r}_2$, and $\vec{r}_s$ are in the same plane along with the origin of the coordinate system (The Earth's center), then we can write as

$$\vec{r}_s = c_1\vec{r}_1 + c_2\vec{r}_2 \tag{29}$$

The values of c_1 and c_2 for each ground site are evaluated using two constraints. The first constraint is the fact that the magnitude of the site position vector $\vec{r}_s$ does not change as Earth is spinning. Hence

$$r_s \equiv \|\vec{r}_s\| = R_E \tag{30}$$

where R_E is the Earth radius. The second constraint is the fact that the z-component of the site position vector $\vec{r}_s$ does not change as Earth is spinning. Hence

$$\vec{r}_s(3) = \vec{r}_{s0}(3) \tag{31}$$

From Eqs. (29) and (31)

$$c_1\vec{r}_1(3) + c_2\vec{r}_2(3) = \vec{r}_{s0}(3) \tag{32}$$

Eq. (30) can be rewritten as

$$\begin{aligned} R_E^2 &\equiv \|\vec{r}_s\|^2 = \|c_1\vec{r}_1 + c_2\vec{r}_2\|^2 \\ &= (c_1\vec{r}_1(1) + c_2\vec{r}_2(1))^2 + (c_1\vec{r}_1(2) + c_2\vec{r}_2(2))^2 \\ &\quad + (c_1\vec{r}_1(3) + c_2\vec{r}_2(3))^2 \end{aligned} \tag{33}$$

Substituting for c_2 from Eq. (32) into Eq. (33) and collecting terms

$$\begin{aligned} &\left(1 + \left(\frac{\vec{r}_1(3)}{\vec{r}_2(3)}\right)^2 - 2\left(\frac{\vec{r}_1(3)}{\vec{r}_2(3)}\right)\cos\vartheta_{12}\right)c_1^2 \\ &\quad + 2\frac{\vec{r}_{s0}(3)}{\vec{r}_2(3)}\left(\cos\vartheta_{12} - \frac{\vec{r}_1(3)}{\vec{r}_2(3)}\right)c_1 \\ &\quad + \left(\frac{\vec{r}_{s0}(3)}{\vec{r}_2(3)}\right)^2 - 1 = 0 \end{aligned} \tag{34}$$

where ϑ_{12} is the angle between $\vec{r}_1$ and $\vec{r}_2$. This is a second order equation in c_1 and yields two solutions. For each solution, Eq. (32) can be used to calculate the corresponding c_2. By substituting with the values of c_1 and c_2 in Eq. (29), two possible intersection position vectors, $\vec{r}_{s1}$ and $\vec{r}_{s2}$, are determined for each ground site.

References

[1] R.H. Battin, An Introduction to the Mathematics and Methods of Astrodynamics, AIAA, 1987.
[2] J. Schaub, H. Junkins, Analytical Mechanics of Space Systems, AIAA, 2003.
[3] B. Wie, Space Vehicle Dynamics and Control, AIAA Educational Series, AIAA, Reston, VA, 1998.
[4] J.R. Wertz, Mission Geometry; Orbit and Constellation Design and Management, Space Technology Library, Springer, 2001.
[5] C. Brown, Spacecraft Mission Design, AIAA, 1998.
[6] J. Wertz, W. Larson, Space Mission Analysis and Design, Microcosm Press, 1999.

[7] M. Netzband, W.L. Stefanov, C. Redman, Applied Remote Sensing for Urban Planning, Governance and Sustainability, Springer, 2007.
[8] D. Whelan, A. Filip, J. Koss, T. Kurien, G. Pappas, Global space-based ground surveillance: mission utility and performance of discoverer II, in: IEEE Aerospace Conference Proceedings, vol. 5, 2000, pp. 1–11.
[9] P. Fortescue, J. Stark, G. Swinerd, Spacecraft Systems Engineering, Wiley, London, UK, 2003.
[10] M. Guelman, A. Kogan, Electric propulsion for remote sensing from low orbits, Journal of Guidance, Control and Dynamics 22 (2) (1999).
[11] O. Abdelkhalik, D. Mortari, Orbit design for ground surveillance using genetic algorithms, Journal of Guidance, Control, and Dynamics 29 (5) (2006) 1231–1235.
[12] B.J. Wall, B.A. Conway, Genetic algorithms applied to the solution of hybrid optimal control problems in astrodynamics, Journal of Global Optimization (4) (2009) 493–508 doi:http://dx.doi.org/10.1007/s10898-008-9352-4.
[13] J.A. Englander, B.A. Conway, B.J. Wall, Optimal strategies found using genetic algorithms for deflecting hazardous near-earth objects, in: CEC'09: Proceedings of the 11th Conference on Congress on Evolutionary Computation, IEEE Press, Piscataway, NJ, USA, 2009, pp. 2309–2315.
[14] O. Abdelkhalik, D. Mortari, Reconnaissance problem using genetic algorithms, in: Paper AAS 05-184 of the 2005 Space Flight Mechanics Meeting Conference, 2005.
[15] O. Abdelkhalik, Initial orbit design from ground track points, Journal of Spacecraft and Rockets 47 (1) (2010) 202–205 AIAA, in print.
[16] H.-D. Kim, O.-C. Jung, H. Bang, A computational approach to reduce the revisit time using a genetic algorithm, in: International Conference on Control, Automation and Systems, 2007, pp. 184–189.
[17] H.-D. Kim, H. Bang, O.-C. Jung, A heuristic approach to the design of an orbit for a temporary reconnaissance mission using a few leo satellites, in: AAS/AIAA Space Flight Mechanics Meeting, January 2008.
[18] E. Williams, W. Crossley, T. Lang, Average and maximum revisit time trade studies for satellite constellations using a multiobjective genetic algorithm, Journal of the Astronautical Sciences (3) (2001) 385–400.
[19] D.A. Vallado, Fundamentals of Astrodynamics and Applications, second ed., Microcosm Press and Kluwer Academic Publications, 2004.
[20] D. Mortari, M.P. Wilkins, C. Bruccoleri, On sun-synchronous orbits and associated constellations, in: Sixth DCSSS Conference, Riomaggiore, Italy, 2004.
[21] A. Gad, O. Abdelkhalik, Repeated shadow track orbits for space-sunsetter missions, International Journal of Aerospace Engineering 2009 (2009) 13pp, Article ID 561495, doi:10.1155/2009/561495.
[22] J.S. Chitode, Power Electronics, Technical Publications, Pune, India, 2008.
[23] D. Goldberg, Genetic Algorithms in Search, Optimization, and Machine Learning, Addison Wesley Longman Inc, 1989.